Electronic Supplementary Material (ESI) for Soft Matter.

Supplementary Information for

Quantifying cooperative flow of fat crystal dispersions

Klaudia W. Milc,[a] Joshua A. Dijksman,[b] John P. M. van Duynhoven [a, c] and Camilla Terenzi [a]

[a]Laboratory of Biophysics, Wageningen University, Wageningen, The Netherlands.
[b]Physical Chemistry and Soft Matter, Wageningen University, Wageningen, The Netherlands.
[c]Unilever Foods Innovation Centre Hive, Wageningen, The Netherlands.

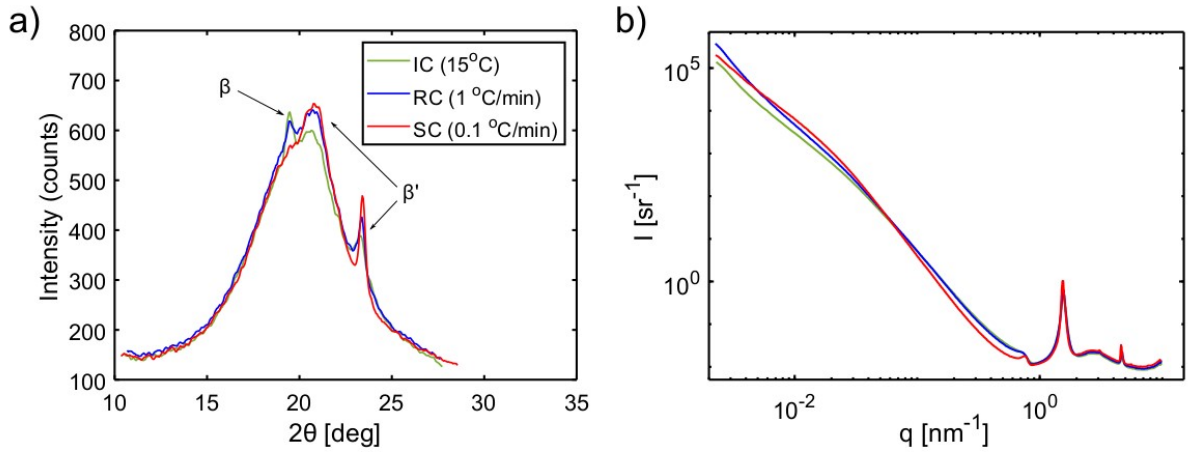

S1. Multiscale structure characterization

Figure S1: *a) WAXD spectra of the three FCD samples evidencing the β′ polymorphic form of the aggregate-forming crystal platelets, for all crystallization rates; b) USAXS intensity, I, as a function of scattering vector, q, with the obtained Porod slope, P_i of 3.1, 3.3 and 2.4 for the FCD samples* ***IC(15)*** *(green),* ***RC(1)*** *(blue) and* ***SC(0.1)*** *(red), respectively.*

Fig. S2 shows the Raman spectra for the FCD samples, acquired in the interstitial spaces between the aggregates, in comparison with the spectrum of a sample consisting solely of the solid fat component of the FCDs. An increase in the intensity of the signals at Raman shifts of 1078 cm^{-1} and 1135 cm^{-1} and a decrease in intensity of the peak at a shift of 1272 cm^{-1} evidences an increasing similarity with the spectrum of pure solid fat, going from sample **IC(15)** towards **SC(0.1)**. This indicates an increase in the solid fat content and in the colloidal network strength with decreasing crystallization rate.

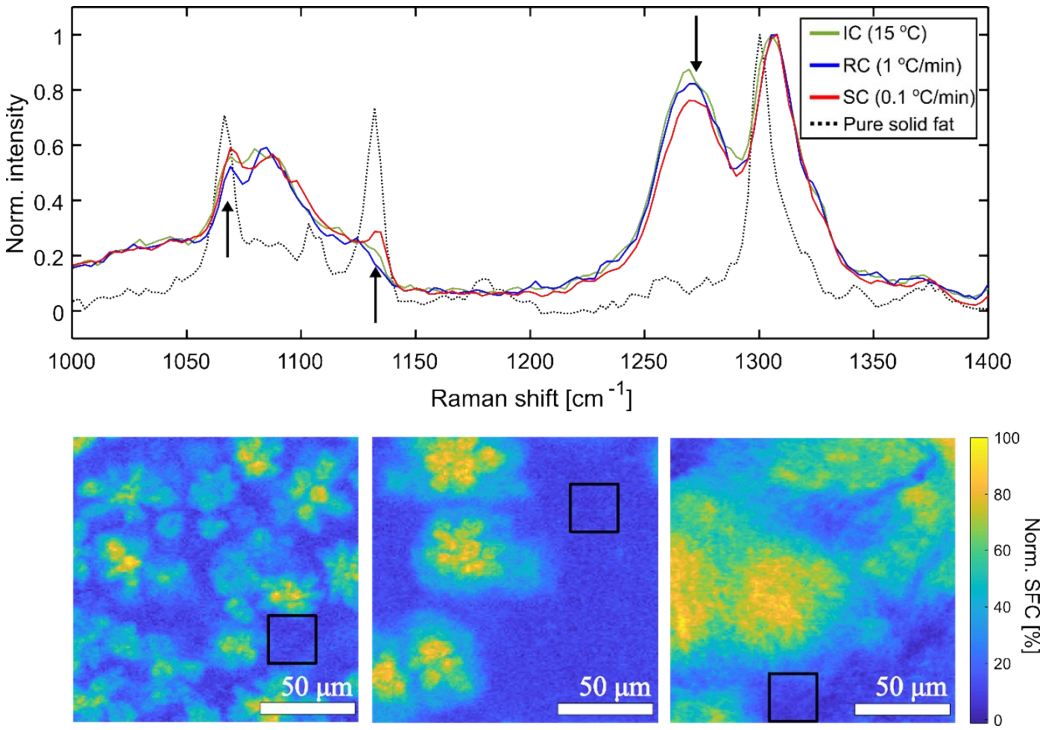

Figure S2: *Raman spectra (top) of the three FCD samples, resulting from averaging of 625 spectra in the interstitial space of 25 x 25 pixels, from the areas marked with black rectangles in the respective Raman*

*images (bottom) of samples **IC(15)** (left), **RC(1)** (middle) and **SC(0.1)** (right). Spectra of the FCDs are compared with the spectrum of pure solid fat (dotted black line).*

S2. Shear rate inhomogeneity in the wide-gap CC

We calibrated the effect of the wide gap condition on the measured stress and shear rate values by acquiring flow curves of a Newtonian fluid, silicone oil, with viscosity, η = 1 Pa s in narrow and wide gap CCs, with respective gap sizes of 0.4 mm and 3.5 mm (data not shown). The calibration yielded an empirical scaling factor of 4 in the applied shear rate, such that $\dot{\gamma}_{narrow} = 4 \times \dot{\gamma}_{wide}$.

In Fig. S3 we present global flow curves for the three FCDs including the correction in the shear rates. The adjusted wide-gap CC global flow data was fitted with the HB model, with the fitting parameters presented in Table S1. Comparing the parameters in Tables S1 and Table 1 we note that only the proportionality constant, A changed as a result of the shear rate correction.

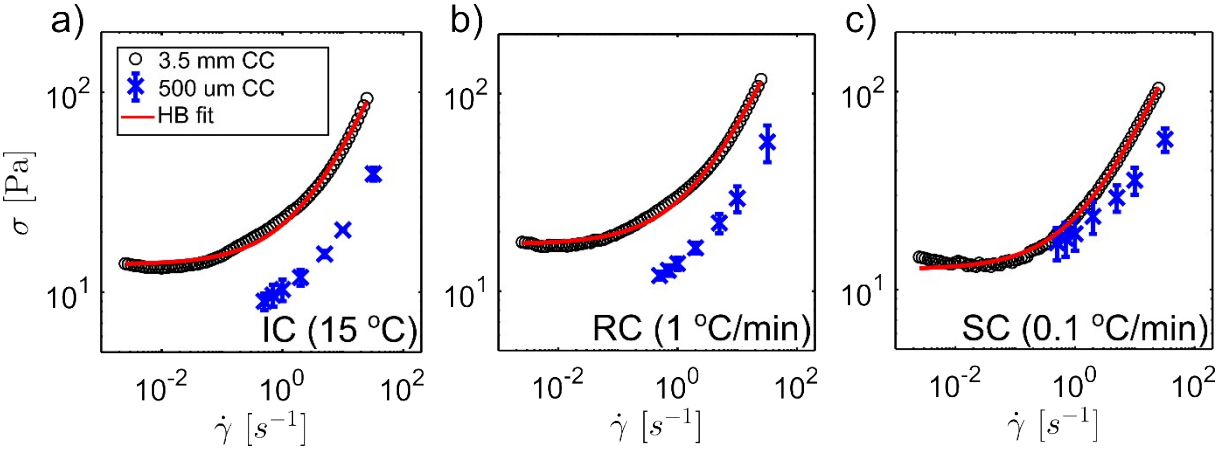

***Figure S3:** Global flow curves of the 27% FCD samples **IC(15)** (a), **RC(1)** (b), and **SC(0.1)** (c) measured with a rheometer, with the stresses acquired in the 3.5 mm gap CC (black circles) plotted against shear rates adjusted for the for the shear rate inhomogeneity caused by the wide gap condition, according to the calibration performed with a Newtonian fluid.*

***Table S1:** Fitting parameters obtained from fitting of the HB model to the global flow curves of the three FCDs adjusted for the shear rate inhomogeneity.*

	σ_y	A	n
IC (15 °C)	13.7 ± 0.2	7.3 ± 0.2	0.70 ± 0.01
RC (1 °C/min)	17.3 ± 0.2	10.3 ± 0.2	0.67 ± 0.01
SC (0.1 °C/min)	12.6 ± 0.1	9.7 ± 0.1	0.67 ± 0.01

S3. Local flow behaviour of the FCDs

The percentage of slip velocity, v_{slip}, shown in Fig. S4, was calculated according to the following equation:

$$v_{slip} = \left(1 - \frac{v_{obs}}{v_{theor}}\right) \times 100 \qquad \text{(S1)}$$

where v_{obs} is the maximum measured velocity and the v_{theor} is the theoretical maximum velocity.

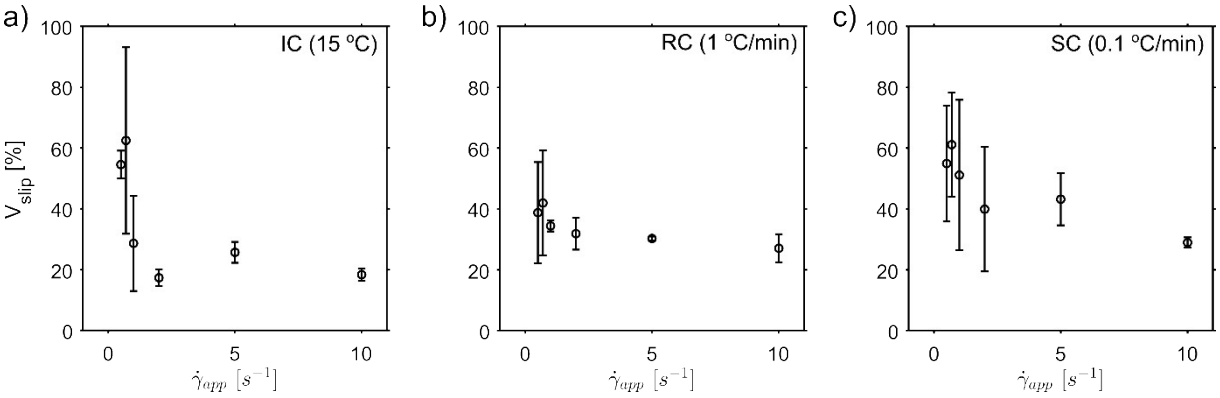

Figure S4: *Mean value of slip velocity at the inner wall, V_{slip}, vs $\dot{\gamma}_{app}$, calculated from the rheo-MRI velocity profiles using Eq. (S1). The error bars is the standard deviation of V_{slip} over three replicate measurements.*

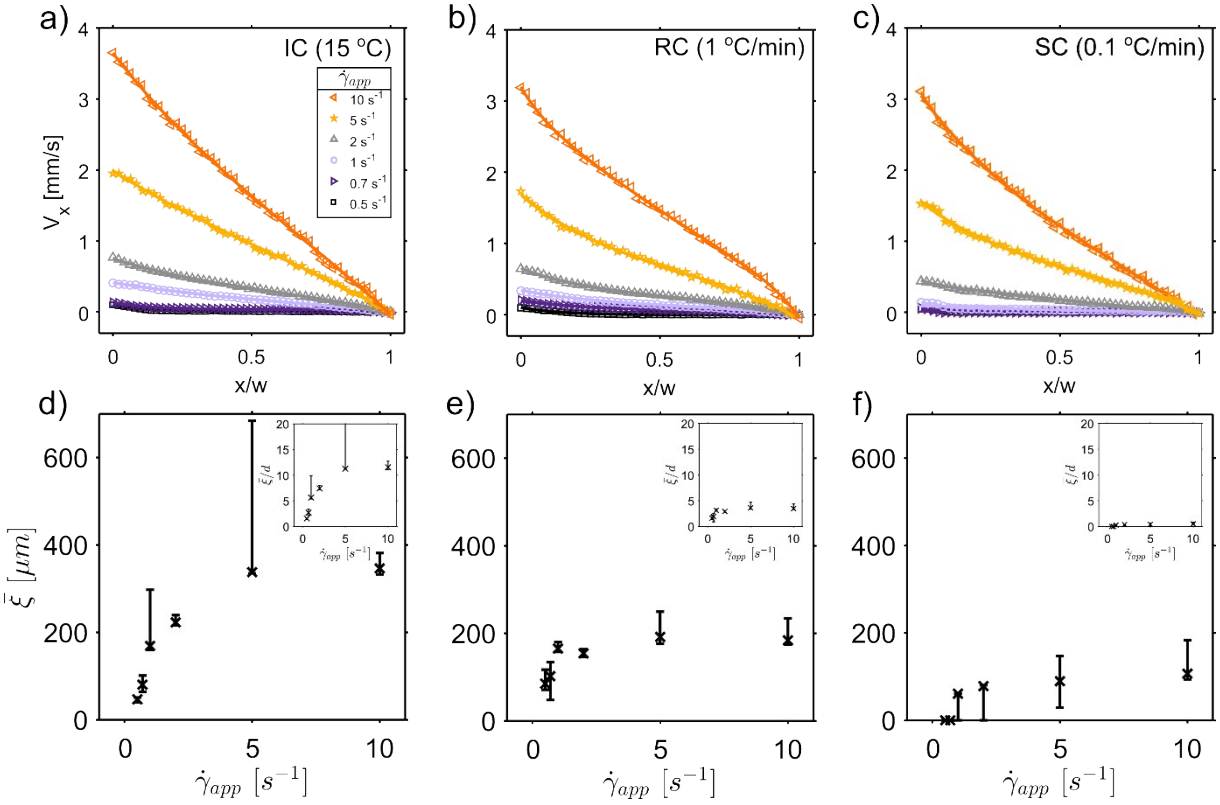

Figure S5*: For samples* ***IC(15)*** *(a and d),* ***RC(1)*** *(b and e) and* ***SC(0.1)*** *(c and f): experimental and fitted velocity profiles (top row) and mean cooperativity lengths, $\bar{\xi}$, (bottom row) obtained from fitting the fluidity model using the bulk flow behaviour adjusted for the shear rate inhomogeneity.*

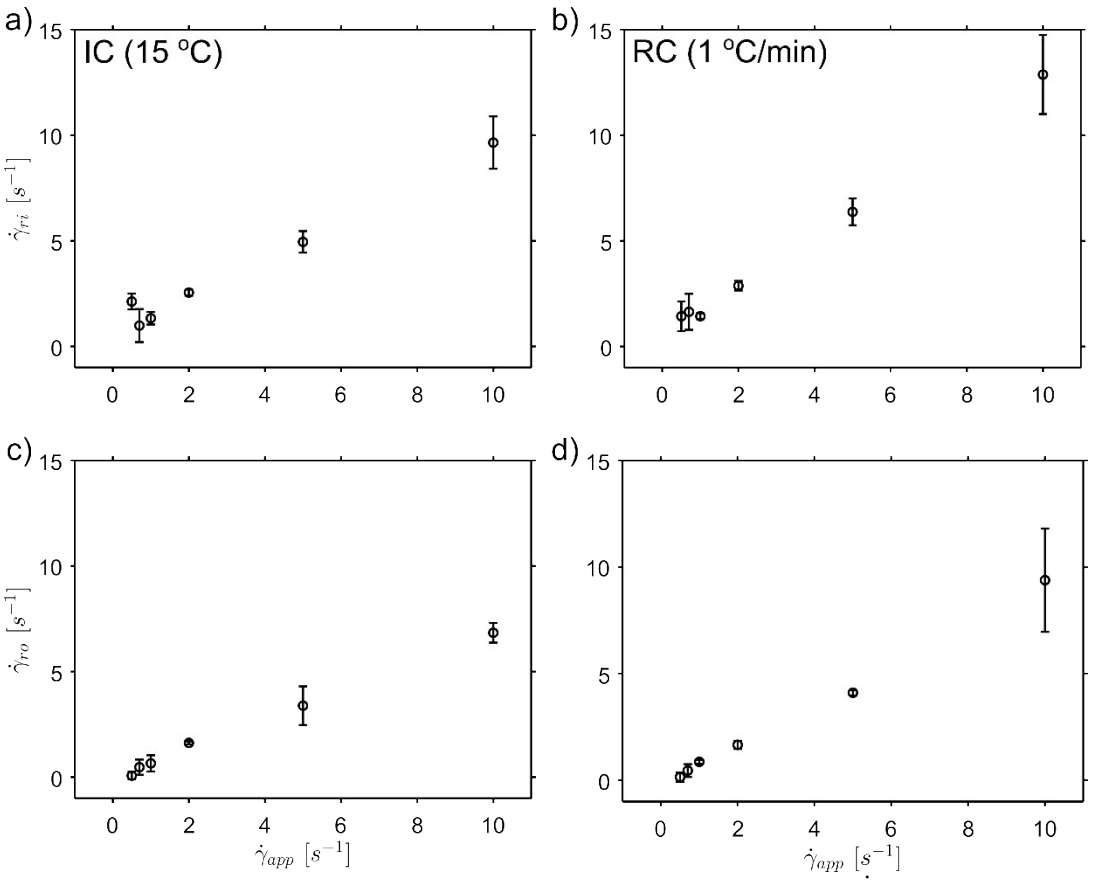

Figure S6: *Plots of the boundary conditions, namely the shear rate at the bob, $\dot{\gamma}_{ri}$ (top), and at the cup, $\dot{\gamma}_{ro}$ (bottom), vs. $\dot{\gamma}_{app}$ obtained from fitting the fluidity model to the rheo-MRI velocity profiles of samples* ***IC(15)*** *(a and c) and* ***RC(1)*** *(b and d). The error bars represent the fitting uncertainty.*